Testing the predictive power of realistic shell model calculations via lifetime measurement of the $11/2^+$ state in ^{131}Sb

S. Bottoni[1,2], E. R. Gamba[1,2], G. De Gregorio[3,4], A. Gargano[4], S. Leoni[1,2], B. Fornal[5],N. Brancadori[1], G. Ciconali[1,2], F. C. L. Crespi[1,2], N. Cieplicka-Oryńczak[5], Ł. W. Iskra[5], G. Colombi[1,2,6], Y.-H. Kim[6], U. Köster[6], C. Michelagnoli[6], F. Dunkel[7], A. Esmaylzadeh[7], L. Gerhard[7], J. Jolie[7], L. Knafla[7], M. Ley[7], J.-M. Régis[7], K. Schomaker[7], M.Sferrazza[8]

[1]*Dipartimento di Fisica, Università degli Studi di Milano, 20133 Milano, Italy*

[2]*INFN Sezione di Milano, 20133, Milano, Italy*

[3]*Dipartimento di Matematica e Fisica, Università degli Studi della Campania "Luigi Vanvitelli," 81100 Caserta, Italy*

[4]*INFN Sezione di Napoli, 80126, Napoli, Italy*

[5]*Institute of Nuclear Physics, PAN, 31-342 Kraków, Poland*

[6]*Institut Laue-Langevin, 38042 Grenoble, France*

[7]*Universität zu Köln, Institut für Kernphysik, 50937 Köln, Germany and*

[8]*Département de Physique, Université libre de Bruxelles, 1050 Bruxelles, Belgium*

(Dated: December 24, 2022)

The lifetime of the $11/2^+_1$ state in the ^{131}Sb nucleus was measured at the LOHENGRIN spectrometer of Institut Laue-Langevin via neutron-induced fission of ^{235}U, using γ-ray fast-timing techniques. The obtained value of $T_{1/2}$=3(2) ps, at the edge of the sensitivity of the experimental method, is the first result for the $11/2^+_1$ state half-life in neutron-rich Sb isotopes. The corresponding quadrupole reduced transition probability to the ground state is B(E2)=$1.4^{+1.5}_{-0.6}$ W.u., indicating a non-collective nature of this state. Realistic shell-model calculations performed in a large valence space reproduce well the experimental value and point to a dominant $2^+(^{130}\mathrm{Sn}) \otimes \pi g_{7/2}$ configuration for the $11/2^+_1$ state, as expected in a weak-coupling scenario. At the same time, the sum of the quadrupole strength of the multiplet states is predicted to exceed the one of the ^{130}Sn core as a consequence of the equal contribution of the proton and the proton-neutron quadrupole matrix elements, pointing to possible development of collectivity already in the close neighborhood of ^{132}Sn.

https://doi.org/10.48733/2023.no2.nz22

I. INTRODUCTION

The emergence of collective excitations and deformations from the single-particle motion is one of the most interesting phenomena in atomic nuclei, the latter being many-body quantum systems made of interacting fermions. Their origin can be traced back to the role of the long-range part of the proton-neutron interaction when it overcomes the resistance power of the spherical-driving paring force (e.g., [1]). The emergence of collectivity is strongly hindered by large energy gaps between single-particle states. However, it has been shown that the monopole part of the nuclear interaction may induce a remodelling of the spacing between single-particle states depending on their occupancies. Such a remodelling may facilitate particle-hole (p-h) excitations with respect to the normal filling of the states. This mechanism is an elegant example of quantum self organization [2–6]. To what extent the proton-neutron interaction prompts the emergence of collectivity is still the subject of many experimental and theoretical studies, being ultimately related to the complex nature of the nuclear forces.

The emergence of collectivity can be investigated moving away from shell closures by a few particles or holes on both proton and neutron sides. Recently, this was studied around two doubly-magic nuclei, namely ^{208}Pb [7] and ^{132}Sn [8], by looking at the low-lying electric quadrupole strengths. In the first case, the $5/2^-_1 \rightarrow 1/2^-$(gs) - E2 decays in $^{209}_{84}$Po, $^{211}_{86}$Rn, and $^{213}_{88}$Ra, were considered, being 2p-1h, 4p-1h, and 6p-1h nuclei with respect to doubly magic $^{208}_{82}\mathrm{Pb}_{126}$. These E2 strengths are expected to be dominated by single neutron-hole transitions with protons acting as spectators. Conversely, a systematic increase of collectivity is observed along the N=125 isotonic chain as more protons are added, indicating the emergence of additional strength beyond the single-hole interpretation. In the second case, the structure of $^{129}_{51}$Sb, with one proton particle coupled to the semimagic $^{128}_{50}\mathrm{Sn}_{78}$ nucleus, was addressed in a Coulomb excitation experiment where the electric quadrupole transition probability for the states of the $2^+(^{128}\mathrm{Sn}) \otimes \pi g_{7/2}$ multiplet was measured. The results point to an increase of collectivity by a factor 1.39(11) compared to the one of the ^{128}Sn core. Shell-model calculations confirm the observed systematic increase of quadrupole collectivity along the N=125 isotonic chain [7] as well as for the multiplet in ^{129}Sb [8], although they underestimate the experimental B(E2) values in both cases.

The observed collectivity enhancement could be ascribed to a constructive quadrupole interference originated by the proton-neutron interaction, going beyond a weak particle - core coupling scheme [9, 10]. In this scheme, one assumes that the low-lying spectrum of the odd-even system is described by coupling the odd nucleon in the lowest allowed orbital to the ground and the yrast 2^+ states of the neighboring semimagic core. In the so-called weak coupling limit, the single particle does not perturb the core and the total quadrupole strength of the multiplet obtained from the 2^+_1 state should be equal to the B(E2 , $0^+ \rightarrow 2^+_1$) value of the

core [9]. This simple description can break down when the particle-core interaction provides extra strength owing to proton-neutron correlations.

The nature of proton-core excitations around ^{132}Sn were investigated by part of this collaboration in ^{133}Sb [11]. No further experimental information is available on the low-lying E2 strength in neutron-rich Sb isotopes except for ^{129}Sb [8], being these nuclei located in an exotic region of the nuclide chart. In this context, the ^{131}Sb nucleus is pivotal to track the emergence of collectivity along the Z=51 isotopic chain as well as to test shell-model interactions, being only 1p-2h away from the double shell closure. The question whether the addition of a single proton to ^{130}Sn, with only two neutron holes, is yet sufficient to produce an enhancement of the quadrupole collectivity is here addressed and discussed in the framework of the shell model.

In this work, the lifetime of the $11/2^+_1$ state in ^{131}Sb was measured by the fast-timing technique [12], the first such result in neutron-rich, odd-even antimony isotopes approaching the N=82 shell closure. This state is expected to be a member of the $2^+(^{130}\mathrm{Sn}) \otimes \pi g_{7/2}$ multiplet, corresponding to the maximum proton-core spin alignment, and decays to the $7/2^+$ ground state via a stretched E2 γ-ray transition. The result yields $T_{1/2}$=3(2) ps, at the limit of sensitivity of the experimental method, and enables to assess the electric-quadrupole reduced transition probability to the ground state, providing $\mathrm{B(E2;}11/2^+_1 \rightarrow 7/2^+_1\mathrm{)}=1.4^{+1.5}_{-0.6}$ W.u, very close to the measured $\mathrm{B(E2;}2^+_1 \rightarrow 0^+_1\mathrm{)}$=1.18(26) W.u of the ^{130}Sn core [13]. The measured $\mathrm{B(E2;}11/2^+_1 \rightarrow 7/2^+_1\mathrm{)}$ value, which, as discussed below, is well reproduced by realistic shell-model calculations, points to an almost pure $2^+(^{130}\mathrm{Sn}) \otimes \pi g_{7/2}$ configuration for the $11/2^+_1$ state. This is somewhat different from the ^{129}Sb case, where a larger fragmentation of the wave function was predicted.

II. THE EXPERIMENT

The experiment was carried out at Institut Laue-Langevin (ILL), by using the LOHENGRIN spectrometer [14]. Antimony-131 nuclei were produced by thermal neutron-induced fission of a 378-μg/cm^2-thick, ^{235}U target, exposed to a neutron flux of 5×10^{14} n·cm^{-2} ·s^{-1}. Recoiling fission fragments were selected combining magnetic and electric fields, separating the ions according to their A/q and E/q, mass-to-charge and energy-to-charge ratios, respectively, then collimated by a refocusing magnet [15] to the focal plane of the spectrometer. Here, fission products were detected by an ionization chamber at an average rate of 5 kHz and their γ decay was measured by two HPGe clover detectors and four $LaBr_3$(Ce), fast scintillators. The latter were arranged in a standard analog fast-timing setup, allowing the measurement of sub-nanosecond lifetimes of excited states via γ-γ coincidence relationships [16]. Given the typical time-of-flight of the ions of about 2 μs from the target to the focal plane, only γ decays stemming from sufficiently long-lived isomeric states are observed at the focal plane of the mass separator. Prior to this work, three isomers were already known in the ^{131}Sb nucleus [17, 18], namely the $(23/2^+)$, $(19/2^-)$, and $(15/2^-)$ states at 2165.6 keV, 1687.2 keV, and 1676.1 keV, with half-lives of 0.97(3), 4.3(8) and 64(3) μs, respectively, the latter adopted from the most recent measurement reported in Ref. [18]. In this context, the $11/2^+_1$ state at 1226 keV is fed by the 450-keV transition, depopulating the 64-μs isomer, and decays directly to the $7/2^+_1$ ground state via the emission of an E2 γ ray. Following detection of fission fragments by the ionization chamber, γ-ray events were built within a 10-μs time-coincidence window. This turned out to be sufficiently wide to measure the 450-1226-keV cascade from the 64-μs isomer in ^{131}Sb with significant statistics, limiting, at the same time, background contamination originating from β^- decays of A=131 isobars. The total projections of the γ-γ matrices measured by HPGe detectors and $LaBr_3$(Ce) scintillators are shown in Fig. 1, in black and red, respectively, where γ lines of ^{131}Sb at 450 keV and 1226 keV are indicated. The superior energy resolution of HPGe crystals enabled to characterize all γ rays observed in the present experiment. In the spectra, the ^{131}Te and ^{131}I γ rays, emitted after the ^{131}Sb β^- decay, appear as random coincidences and are labeled accordingly. The selectivity achieved in this experiment on the 450-1226-keV cascade in ^{131}Sb was verified by gat-

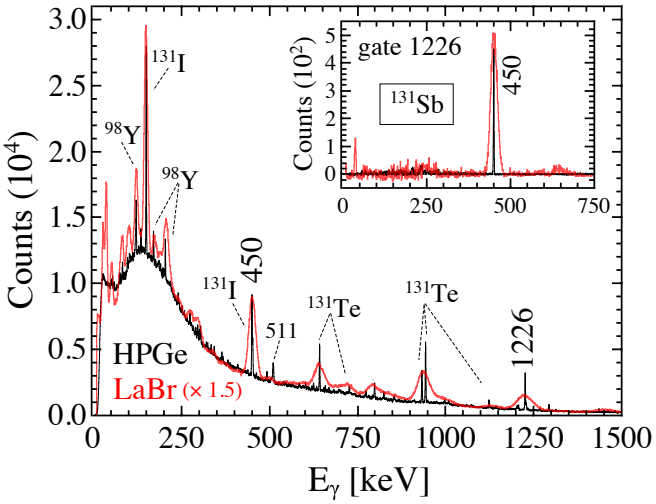

FIG. 1. (Color online) Total projections of the γ-γ matrices measured by HPGe detectors (black) and $LaBr_3$(Ce) scintillators (red). The 450- and 1226-keV transitions in ^{131}Sb, populating and depopulating the $11/2^+$ state, respectively, are highlighted. The γ lines coming from β^- decays are also marked (see text for details). (Inset) Projection of the γ-γ matrices gated on the 1226-keV transition in ^{131}Sb, showing a clean coincidence with the 450-keV line de-exciting the 64-μs isomer.

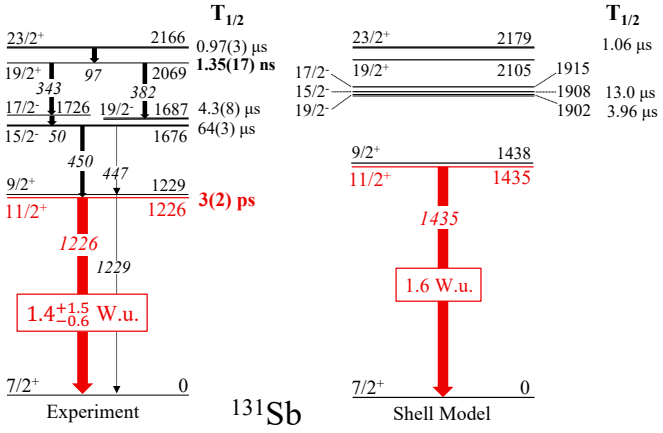

FIG. 2. (Color online) Left: partial experimental level scheme of ^{131}Sb, as observed in this work, with the $11/2^+_1$ state and its E2 decay (of interest here) shown in red. The $T_{1/2}$=3(2) ps half-life of the $11/2^+$ state and the $T_{1/2}$=1.35(17) ns half-life of the $19/2^+$ measured in this experiment are reported in bold, together with literature values for the microsecond isomers, taken from [18]. Right: Realistic shell model predictions obtained using the V_{low-k} approach (see text for details). The experimental and theoretical B(E2;$11/2^+_1 \rightarrow 7/2^+_1$) values are also displayed.

ing on the 1226-keV line, as illustrated in the inset of Fig. 1. The background-subtracted projected spectrum shows a clean coincidence with the 450-keV γ ray only, for both HPGe and $LaBr_3$(Ce) detectors. At low energy, also lines of the strongly produced microsecond isomer in ^{98}Y [19], reaching the focal plane with a similar A/q ratio as A=131 ions, are observed. However, these low-energy lines do not interfere with the 1226-keV gate and no additional ion energy gating was required. It is important to note that the 64-μs isomer in ^{131}Sb also feeds the $9/2^+$ state at 1229 keV with a γ-ray branch of 3%. The possible interference of the 447-1229 keV coincidence was addressed by analysing the $\gamma-\gamma$ coincidence matrix measured with HPGe detectors, yet showing a contribution of less than 1% in the coincident spectrum.

III. DATA ANALYSIS

The decay scheme of ^{131}Sb, as observed in this work, is reported in Fig. 2 left. The lifetime of the $11/2^+$ state was measured by using the *generalized centroid difference* (GCD) method [20], applied to the 450-1226-keV, feeding-decay (E_f,E_d) cascade. For this purpose, $LaBr_3$(Ce) scintillator events were sorted into E_γ-E_γ-Δt cubes, with the first and second energy axis carrying the start and stop signals, respectively. Delayed (D) and antidelayed (AD) time distributions were obtained by projecting to the time axis the E_γ-E_γ, start-stop matrix, gated on the 450-1226-keV coincidence in the D and AD sectors. This procedure is presented in panel a) of Fig. 3 for the delayed case, where the coincident events are marked in red and labelled as p|p. The projected time distribution is shown in panel b). In order to investigate possible sources of background originating from γ-ray Compton scattering and random coincidences, the method introduced in Ref. [21] and successfully applied in Refs. [22–24] was employed. Three different pairs of background regions on both the D and AD sides were identified and selected around the 450-1226-keV coincidence peaks. These contributions are evaluated from the p|b, peak-background, b|p, background-peak, and b|b, background-background regions, shown in Fig. 3 a) and highlighted in green, purple and gold, respectively. The *true* centroid positions of the D and AD time distributions were obtained by the deconvolution of the p|p, p|b, b|p, and b|b components, as

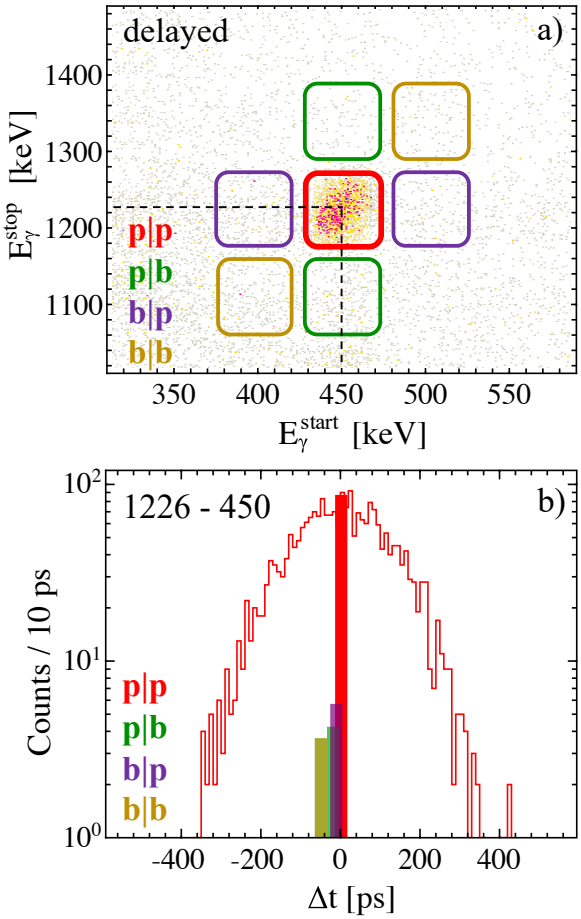

FIG. 3. (Color online) Panel a): start-stop γ-γ matrix measured by $LaBr_3$(Ce) scintillators. The energy gate around the 450-1226-keV, p|p coincidence is marked in red and corresponds to the delayed sector. The p|b, b|p, and b|b background gates are shown in green, purple, and gold, respectively (see text for details). Panel b): delayed time distributions for the 450-1226-keV cascade. Vertical bars represent the centroid positions of the p|p (red), p|b (green), b|p (purple), and b|b (gold) components, with their height being proportional to the number of counts in each time distribution.

described in Ref. [22]. This is schematically illustrated in Fig. 3 b), adopting the graphical concept introduced in Ref. [23]. Vertical bars are centered around the centroid positions of the p|p, p|b, p|b, and b|b time distributions, their height proportional to the number of counts in each component. Similar results were obtained for the antidelayed case. Finally, the lifetime of the $11/2^+$ state was obtained by $2\tau = \Delta$C-PRD(E_f,E_d), where ΔC is the centroid difference between the D and AD time distributions and the PRD(E_f,E_d) correction is the so-called *prompt response difference*, which accounts for time-walk effects in $LaBr_3$(Ce) detectors [20]. In this work, the PRD calibration was precisely measured as a function of γ-ray energy by using a ^{152}Eu source and ^{187}W and ^{185}Os sources specifically produced at ILL to include low-energy data points [16]. The result for the lifetime of the $11/2^+$ state is τ=5(3) ps, corresponding to $T_{1/2}$=3(2) ps. All together, this measurement represents a remarkable example of the finest accuracy achievable with this experimental technique, at the limit of applicability of the GCD method. Other examples of short lifetimes measured with this technique can be found in Refs. [25–27]. The reduced transition probability for the 1226-keV, E2 γ decay from the $11/2^+$ state was deduced from the measured lifetime, its value being B(E2;$11/2^+_1 \rightarrow 7/2^+_1$)=$1.4^{+1.5}_{-0.6}$ W.u. For the sake of completeness, we report the lifetime of the $19/2^+$ state at 2069 keV in ^{131}Sb, which was also measured in this experiment. In this case, statistics was enhanced by applying gates on both the $19/2^+ \rightarrow 17/2^-$ and $19/2^+ \rightarrow 19/2^-$ decaying transitions, the time difference of which was considered with respect to the 97-keV $23/2^+ \rightarrow 19/2^+$ feeding transition. Contrary to the $11/2^+$ case, the measured time distributions showed clear tails pointing to a longer lifetime for this state. The background was subtracted following the procedure reported in [28] for both the D and AD time distributions. The lifetime was extracted with the so-called convolution method using a Gaussian distribution and an exponential decay [29]. The weighted average lifetime obtained from the separate analysis of the D and AD time distributions is τ = 1944(246) ps, corresponding to $T_{1/2}$=1347(171) ps.

IV. DISCUSSION

In order to get a better insight into the experimental results, we have performed realistic shell-model calculations using the KSHELL code [30]. We have considered ^{100}Sn as closed inert core with protons and neutrons in the valence space made up by the $0g_{7/2}$, $1d_{5/2}$, $1d_{3/2}$, $2s_{1/2}$ and $0h_{11/2}$ orbitals for both protons and neutrons. The two-body effective interaction was derived within the framework of many-body perturbation theory from the CD-Bonn nucleon-nucleon potential [31] renormalized by way of the V_{low-k} approach [32] with the addition of the Coulomb potential. In particular, we have adopted the $\hat{Q}$ - box folded-diagram approach [33], including in the perturbative expansion of the $\hat{Q}$ - box one and two-body diagrams up to the third order in the interaction. The effective charges adopted for the E2 operator are $e_p = 1.7e$ and $e_n = 0.67e$, chosen to reproduce the experimental B(E2; $2^+_1 \rightarrow 0^+_1$) = 31.5(1.0) and 1.18(26) W.u. of ^{134}Te and ^{130}Sn, respectively. This is done consistently with the procedure adopted in the ^{129}Sb case [8], described within the same theoretical framework here discussed, where $e_n = 0.9e$ was used to fit the B(E2) of the ^{128}Sn core [34]. The partial experimental level and decay scheme of ^{131}Sb is compared to shell-model calculations in Fig. 2, where only the states observed in this work are reported. A good agreement is obtained in terms of spin-parity sequences and the energies of the $23/2^+$ and $19/2^+$ are correctly reproduced, while the negative-parity states and the $11/2^+$ state are overestimated by $\sim$ 200 keV. Shell-model calculations were also performed for the half lives of the $23/2^+$, $19/2^-$, and $15/2^-$ isomeric states, yielding 1.06, 3.96 and 13 μs, respectively. For the $15/2^-$ state, we have considered the $15/2^- \rightarrow 11/2^+$ M2 transition, using g-factor standard values. The $11/2^+_1$ state and its E2 γ decay is shown in red in Fig. 2. The predicted B(E2;$11/2^+_1 \rightarrow 7/2^+_1$)=1.6 W.u. is found in perfect agreement with the experimental value of $1.4^{+1.5}_{-0.6}$ W.u. obtained in this work. The calculated wave function of the $11/2^+_1$ state is dominated by the $2^+(^{130}\text{Sn}) \otimes \pi g_{7/2}$ configuration (88%). Similarly, the $7/2^+$ ground state is predicted to be characterized by the single main component $0^+(^{130}\text{Sn}) \otimes \pi g_{7/2}$. As anticipated earlier, our result is very close to the B(E2;$2^+_1 \rightarrow 0^+_1$)=1.18(26) W.u of the ^{130}Sn core [13]. This, along with shell-model predictions pointing to an almost pure proton-core coupling scheme for both the $7/2^+_1$ and $11/2^+_1$ states, suggests that the extra $g_{7/2}$ proton does not perturb the ^{130}Sn core, with no enhancement of quadrupole strength in the decay of the $11/2^+_1$ state. In the case of the 1p-4h ^{129}Sb [8] isotope, a B(E2;$11/2^+_1 \rightarrow 7/2^+_1$) value of 7.5(5) W.u. is reported, already exceeding the B(E2;$2^+_1 \rightarrow 0^+_1$)=4.2(3) W.u of the ^{128}Sn core [34]. This is partially predicted by shell-model calculations, with a calculated B(E2;$11/2^+_1 \rightarrow 7/2^+_1$) of 5.1 W.u., yet smaller than the experimental one.

The systematic of the 2^+ and of the $11/2^+$ states in Sn and Sb isotopes, respectively, is presented in Fig. 4 in terms of energy (top) and B(E2) values (bottom), for both experimental data and shell-model calculations. While the experimental energies of the $11/2^+$ states follow the same constant trend of the 2^+ states of the Sn cores, the quadrupole reduced transition probabilities increase from ^{131}Sb to ^{129}Sb, compared to the corresponding even-even Sn cores. This enhancement is predicted by shell-model calculations and can be attributed to i) a larger fragmentation of the wave function of the $11/2^+$ state and ii) a coherent interference of the proton-neutron terms in the quadrupole strength. However, the experimental B(E2; $11/2^+_1 \rightarrow 7/2^+_1$) in ^{129}Sb is slightly underestimated by theory, and this is most likely due to

missing correlations in the shell-model space that come into play when moving away from the shell closure. For N<78, based on our calculations, we should expect even a larger increase of collectivity in the even-odd systems compared to the Sn cores, indicating a more important breakdown of the particle-core weak-coupling limit. According to calculations, this is ascribed to proton-neutron coherent correlations which become larger towards mid shell.

For a better understanding of the effects produced by the proton addition, experimental information on the other multiplet states with spins $3/2^+$, $5/2^+$, $7/2^+$, and $9/2^+$ would be needed. Considering the lack of the experimental data on these multiplet members, we could investigate the validity of the B(E2) sum rule only theoretically. Such predictions would also be a useful guide for future experiments. Based on the weak coupling limit, the sum of the B(E2, $7/2_1^+ \rightarrow j^\pi$) values over all the multiplet states should be equal to the B(E2; $0^+ \rightarrow 2^+$) of the ^{130}Sn core. To verify this, the whole $2^+(^{130}\mathrm{Sn}) \otimes \pi g_{7/2}$ multiplet was calculated within the shell-model framework here discussed, the results being presented in Fig. 5. The excitation energies of these states are known in the literature and they are well reproduced by theory with a χ^2 value of 0.198, but, except for the $9/2^+$ and $11/2^+$ states, they are not populated in the present experiment as they are not fed by any isomeric decay. In Fig. 5, the percentages of the dominant wave-function components are shown in red. The $5/2_1^+$ state is also reported, which is predicted to originate mostly from the $0^+(^{130}\mathrm{Sn}) \otimes \pi d_{5/2}$ coupling, with only a small component coming from the coupling with the 2^+ excitation. In Fig. 5, the calculated B(E2, $7/2_1^+ \rightarrow j^\pi$) are presented in Weisskopf units. Their sum gives 9.2 W.u., to be compared with the experimental B(E2; $0^+ \rightarrow 2^+$)=6.0(15) e^2fm^4 of the ^{130}Sn core [13], thus suggesting an enhancement of the total quadrupole collectivity already in the 1p-2h, ^{131}Sb nucleus. This is in contrast with the expectation of a pure weak coupling scheme. A similar result was found in the case of ^{129}Sb, where the calculated factor is 1.3 [8]. By examining the proton and neutron contributions to the E2 strength, as calculated in this work, we note that the neutron term does not change when passing from ^{130}Sn to ^{131}Sb. Its contribution to the total strength in ^{131}Sb is 66% only, the rest being equally shared between the proton and the proton-neutron interference terms. Also in the case of ^{129}Sb, the neutron contribution is close to that of ^{128}Sn but the enhancement of collectivity originates mainly from the proton-neutron interference term. This effect might be ascribed to a larger wave-function fragmentation of the multiplet states in ^{129}Sb, compared to the ^{131}Sb isotope here discussed.

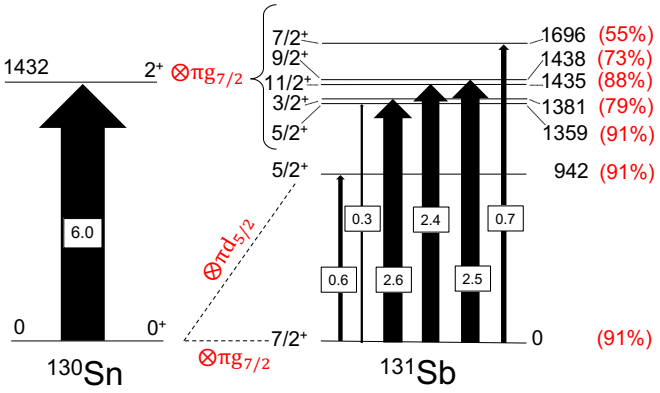

FIG. 5. (Color online) (Left) Shell-model calculations of the 2^+ state and of the B(E2;$0_1^+ \rightarrow 2_1^+$) in ^{130}Sn. (Right) Shell-model calculations of the $2^+(^{130}\mathrm{Sn}) \otimes \pi g_{7/2}$ multiplet in ^{131}Sb and of the B(E2, $7/2_1^+ \rightarrow j^\pi$) in ^{131}Sb. The $5/2_1^+$ state of $0^+(^{130}\mathrm{Sn}) \otimes \pi d_{5/2}$ character, located at 942 keV, is also reported. The percentages of the main wave-function components are indicated in red. Reduced transition probabilities are in Weisskopf units (see text for details).

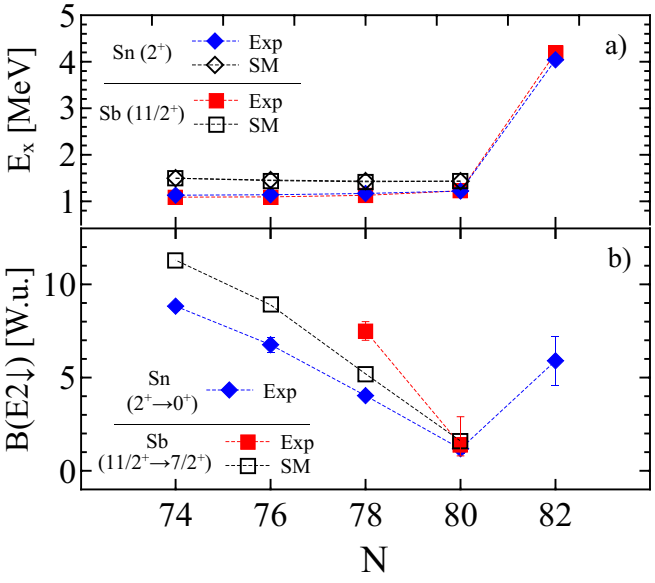

FIG. 4. (Color online) (Top) Systematic of the energy of the 2_1^+ states in Sn isotopes (blue diamonds), compared to the energy of the $11/2_1^+$ states in Sb nuclei (red squares). Realistic shell-model calculations are shown as open diamonds and squares for Sn and Sb nuclei, respectively. (Bottom) Systematic of the B(E2;$2_1^+ \rightarrow 0_1^+$) values in Sn isotopes (blue diamonds), compared to the B(E2; $11/2_1^+ \rightarrow 7/2_1^+$) value in ^{131}Sb obtained in this work (red square). Result for ^{129}Sb are also shown [8]. Realistic shell-model calculations are presented as open squares for Sb nuclei. Calculations for B(E2; $2_1^+ \rightarrow 0_1^+$) values in Sn isotopes are not reported since the effective charges were fitted to reproduce experimental data (see text for details).

V. CONCLUSIONS

In conclusion, the lifetime of the $11/2_1^+$ state in the neutron-rich ^{131}Sb nucleus was measured for the first time by neutron-induced fission of ^{235}U and the γ-ray fast-timing technique at the LOHENGRIN spectrometer of Institut Laue-Langevin, following the decay of μs isomers in ^{131}Sb. The exceptional selectivity achieved in this work for the γ decay of the $11/2_1^+$ state enabled to obtain a half life of 3(2) ps, at the limit of applicability of the experimental technique. The deduced B(E2) transition probability of $1.4^{+1.5}_{-0.6}$ W.u., that is well reproduced by realistic shell-model calculations, equals the one of the ^{130}Sn core. This result points to a non-collective structure of the $11/2_1^+$ state with a dominant $2^+(^{130}\mathrm{Sn}) \otimes \pi g_{7/2}$ configuration, in contrast with ^{129}Sb, where the B(E2; $11/2_1^+ \rightarrow 7/2_1^+$) value exceeds the one of the ^{128}Sn core. In this connection, we have found instructive to predict the other members of the $2^+(^{130}\mathrm{Sn}) \otimes \pi g_{7/2}$ multiplet in ^{131}Sb within the shell-model framework, which accounts for the increased transition strength in ^{129}Sb, albeit only partially. Our shell-model calculations indicate an enhancement of the total quadrupole collectivity already in the 2h-1p system compared to the even-even ^{130}Sn core. Further experimental information on the other multiplet states with spins $3/2^+$, $5/2^+$, $7/2^+$, and $9/2^+$ would be instrumental to validate the shell-model predictions.

ACKNOWLEDGMENTS

This work was supported in part by the Italian Istituto Nazionale di Fisica Nucleare, the Polish National Science Centre, Poland, under research project No. 2020/39/D/ST2/03510, the Polish National Agency for Academic Exchange (NAWA) within the Bekker programme under grant PPN/BEK/2020/1/00431/U/00001, the Institute for Basic Science (IBS-R031-D1), the German DFG under grant JO391/18-1, and the Fonds de la Recherche Scientifique - FNRS under grants numbers J.0174.22 and 4.45.10.08.

[1] I. Talmi, Rev. Mod. Phys. **34**, 704 (1962).
[2] T. Otsuka, Y. Tsunoda, T. Togashi, N. Shimizu, and T. Abe, Journal of Physics: Conference Series **966**, 012027 (2018).
[3] T. Otsuka, A. Gade, O. Sorlin, T. Suzuki, and Y. Utsuno, Rev. Mod. Phys. **92**, 015002 (2020).
[4] Y. Tsunoda, T. Otsuka, N. Shimizu, M. Honma, and Y. Utsuno, Phys. Rev. C **89**, 031301 (2014).
[5] S. Leoni, B. Fornal, N. Mărginean, M. Sferrazza, Y. Tsunoda, T. Otsuka, G. Bocchi, F. C. L. Crespi, A. Bracco, S. Aydin, M. Boromiza, D. Bucurescu, N. Cieplicka-Oryńczak, C. Costache, S. Călinescu, N. Florea, D. G. Ghiţă, T. Glodariu, A. Ionescu, L. Iskra, M. Krzysiek, R. Mărginean, C. Mihai, R. E. Mihai, A. Mitu, A. Negreţ, C. R. Niţă, A. Olăcel, A. Oprea, S. Pascu, P. Petkov, C. Petrone, G. Porzio, A. Şerban, C. Sotty, L. Stan, I. Ştiru, L. Stroe, R. Şuvăilă, S. Toma, A. Turturică, S. Ujeniuc, and C. A. Ur, Phys. Rev. Lett. **118**, 162502 (2017).
[6] N. Mărginean, D. Little, Y. Tsunoda, S. Leoni, R. V. F. Janssens, B. Fornal, T. Otsuka, C. Michelagnoli, L. Stan, F. C. L. Crespi, C. Costache, R. Lica, M. Sferrazza, A. Turturica, A. D. Ayangeakaa, K. Auranen, M. Barani, P. C. Bender, S. Bottoni, M. Boromiza, A. Bracco, S. Călinescu, C. M. Campbell, M. P. Carpenter, P. Chowdhury, M. Ciemała, N. Cieplicka-Oryńczak, D. Cline, C. Clisu, H. L. Crawford, I. E. Dinescu, J. Dudouet, D. Filipescu, N. Florea, A. M. Forney, S. Fracassetti, A. Gade, I. Gheorghe, A. B. Hayes, I. Harca, J. Henderson, A. Ionescu, L. W. Iskra, M. Jentschel, F. Kandzia, Y. H. Kim, F. G. Kondev, G. Korschinek, U. Köster, Krishichayan, M. Krzysiek, T. Lauritsen, J. Li, R. Mărginean, E. A. Maugeri, C. Mihai, R. E. Mihai, A. Mitu, P. Mutti, A. Negret, C. R. Niţă, A. Olăcel, A. Oprea, S. Pascu, C. Petrone, C. Porzio, D. Rhodes, D. Seweryniak, D. Schumann, C. Sotty, S. M. Stolze, R. Şuvăilă, S. Toma, S. Ujeniuc, W. B. Walters, C. Y. Wu, J. Wu, S. Zhu, and S. Ziliani, Phys. Rev. Lett. **125**, 102502 (2020).
[7] M. Gerathy, A. Mitchell, G. Lane, A. Stuchbery, A. Akber, H. Alshammari, L. Bignell, B. Coombes, J. Dowie, T. Gray, T. Kibédi, B. McCormick, L. McKie, M. Rahman, M. Reece, N. Spinks, B. Tee, Y. Zhong, and K. Zhu, Physics Letters B **823**, 136738 (2021).
[8] T. J. Gray, J. M. Allmond, A. E. Stuchbery, C.-H. Yu, C. Baktash, A. Gargano, A. Galindo-Uribarri, D. C. Radford, J. C. Batchelder, J. R. Beene, C. R. Bingham, L. Coraggio, A. Covello, M. Danchev, C. J. Gross, P. A. Hausladen, N. Itaco, W. Krolas, J. F. Liang, E. Padilla-Rodal, J. Pavan, D. W. Stracener, and R. L. Varner, Phys. Rev. Lett. **124**, 032502 (2020).
[9] A. de Shalit, Phys. Rev. **122**, 1530 (1961).
[10] A. Bohr and B. Mottelson, *Nuclear Structure*, Vol. II: Nuclear Deformation (W. A. Benjamin, New York, 1975).
[11] G. Bocchi, S. Leoni, B. Fornal, G. Colò, P. Bortignon, S. Bottoni, A. Bracco, C. Michelagnoli, D. Bazzacco, A. Blanc, G. de France, M. Jentschel, U. Köster, P. Mutti, J.-M. Régis, G. Simpson, T. Soldner, C. Ur, W. Urban, L. Fraile, R. Lozeva, B. Belvito, G. Benzoni, A. Bruce, R. Carroll, N. Cieplicka-Oryczak, F. Crespi, F. Didierjean, J. Jolie, W. Korten, T. Kröll, S. Lalkovski, H. Mach, N. Mărginean, B. Melon, D. Mengoni, B. Million, A. Nannini, D. Napoli, B. Olaizola, V. Paziy, Z. Podolyák, P. Regan, N. Saed-Samii, B. Szpak, and V. Vedia, Physics Letters B **760**, 273 (2016).
[12] H. Mach, R. Gill, and M. Moszyński, Nuclear Instruments and Methods in Physics Research Section A: Accelerators, Spectrometers, Detectors and Associated Equipment **280**, 49 (1989).

[13] B. Pritychenko, E. Běták, M. Kellett, B. Singh, and J. Totans, Nuclear Instruments and Methods in Physics Research Section A: Accelerators, Spectrometers, Detectors and Associated Equipment **640**, 213 (2011).

[14] P. Armbruster, M. Asghar, J. Bocquet, R. Decker, H. Ewald, J. Greif, E. Moll, B. Pfeiffer, H. Schrader, F. Schussler, G. Siegert, and H. Wollnik, Nucl. Instrum. Methods **139**, 213 (1976).

[15] G. Fioni, H. Faust, M. Gross, M. Hesse, P. Armbruster, F. Gönnenwein, and G. Münzenberg, Nucl. Instrum. Methods Phys. Res., Sect. A **332**, 175 (1993).

[16] J.-M. Régis, A. Esmaylzadeh, J. Jolie, V. Karayonchev, L. Knafla, U. Köster, Y. Kim, and E. Strub, Nuclear Instruments and Methods in Physics Research Section A: Accelerators, Spectrometers, Detectors and Associated Equipment **955**, 163258 (2020).

[17] J. Genevey, J. A. Pinston, H. Faust, C. Foin, S. Oberstedt, and M. Rejmund, Eur. Phys. J. A **9**, 191 (2000).

[18] S. Biswas, A. Lemasson, M. Rejmund, A. Navin, Y. H. Kim, C. Michelagnoli, I. Stefan, R. Banik, P. Bednarczyk, S. Bhattacharya, S. Bhattacharyya, E. Clément, H. L. Crawford, G. de France, P. Fallon, G. Frémont, J. Goupil, B. Jacquot, H. J. Li, J. Ljungvall, *et al.*, Phys. Rev. C **99**, 064302 (2019).

[19] W. Urban, M. Czerwiński, J. Kurpeta, T. Rzaca-Urban, J. Wiśniewski, T. Materna, L. W. Iskra, A. G. Smith, I. Ahmad, A. Blanc, H. Faust, U. Köster, M. Jentschel, P. Mutti, T. Soldner, G. S. Simpson, J. A. Pinston, G. de France, C. A. Ur, V.-V. Elomaa, T. Eronen, J. Hakala, A. Jokinen, A. Kankainen, I. D. Moore, J. Rissanen, A. Saastamoinen, J. Szerypo, C. Weber, and J. Äystö, Phys. Rev. C **96**, 044333 (2017).

[20] J.-M. Régis, H. Mach, G. Simpson, J. Jolie, G. Pascovici, N. Saed-Samii, N. Warr, A. Bruce, J. Degenkolb, L. Fraile, C. Fransen, D. Ghita, S. Kisyov, U. Koester, A. Korgul, S. Lalkovski, N. Mărginean, P. Mutti, B. Olaizola, Z. Podolyák, *et al.*, Nucl. Instrum. Methods Phys. Res., Sect. A **726**, 191 (2013).

[21] E. Gamba, A. Bruce, and M. Rudigier, Nucl. Instrum. Methods Phys. Res., Sect. A **928**, 93 (2019).

[22] E. R. Gamba, A. M. Bruce, S. Lalkovski, M. Rudigier, S. Bottoni, M. P. Carpenter, S. Zhu, J. T. Anderson, A. D. Ayangeakaa, T. A. Berry, I. Burrows, M. C. Gallardo, R. J. Carroll, P. Copp, D. M. Cullen, T. Daniel, G. F. Martínez, J. P. Greene, L. A. Gurgi, *et al.*, Phys. Rev. C **100**, 044309 (2019).

[23] M. Rudigier, P. Walker, R. Canavan, Z. Podolyák, P. Regan, P.-A. Söderström, M. Lebois, J. Wilson, N. Jovancevic, A. Blazhev, J. Benito, S. Bottoni, M. Brunet, N. Cieplicka-Oryńczak, S. Courtin, D. Doherty, L. Fraile, K. Hadyńska-Klek, M. Heine, L. Iskra, *et al.*, Phys. Lett. B **801**, 135140 (2020).

[24] R. L. Canavan, M. Rudigier, P. H. Regan, M. Lebois, J. N. Wilson, N. Jovancevic, P.-A. Söderström, S. M. Collins, D. Thisse, J. Benito, S. Bottoni, M. Brunet, N. Cieplicka-Oryńczak, S. Courtin, D. T. Doherty, L. M. Fraile, K. Hadyńska-Klek, G. Häfner, M. Heine, L. W. Iskra, *et al.*, Phys. Rev. C **101**, 024313 (2020).

[25] A. Esmaylzadeh, L. M. Gerhard, V. Karayonchev, J.-M. Régis, J. Jolie, M. Bast, A. Blazhev, T. Braunroth, M. Dannhoff, F. Dunkel, C. Fransen, G. Häfner, L. Knafla, M. Ley, C. Müller-Gatermann, K. Schomacker, N. Warr, and K.-O. Zell, Phys. Rev. C **98**, 014313 (2018).

[26] L. Knafla, G. Häfner, J. Jolie, J.-M. Régis, V. Karayonchev, A. Blazhev, A. Esmaylzadeh, C. Fransen, A. Goldkuhle, S. Herb, C. Müller-Gatermann, N. Warr, and K. O. Zell, Phys. Rev. C **102**, 044310 (2020).

[27] L. Knafla, P. Alexa, U. Köster, G. Thiamova, J.-M. Régis, J. Jolie, A. Blanc, A. M. Bruce, A. Esmaylzadeh, L. M. Fraile, G. de France, G. Häfner, S. Ilieva, M. Jentschel, V. Karayonchev, W. Korten, T. Kröll, S. Lalkovski, S. Leoni, H. Mach, N. Mărginean, P. Mutti, G. Pascovici, V. Paziy, Z. Podolyák, P. H. Regan, O. J. Roberts, N. Saed-Samii, G. S. Simpson, J. F. Smith, T. Soldner, C. Townsley, C. A. Ur, W. Urban, A. Vancraeyenest, and N. Warr, Phys. Rev. C **102**, 054322 (2020).

[28] V. Werner, N. Cooper, J.-M. Régis, M. Rudigier, E. Williams, J. Jolie, R. B. Cakirli, R. F. Casten, T. Ahn, V. Anagnostatou, Z. Berant, M. Bonett-Matiz, M. Elvers, A. Heinz, G. Ilie, D. Radeck, D. Savran, and M. K. Smith, Phys. Rev. C **93**, 034323 (2016).

[29] K. Lan and J. W. Jorgenson, Journal of Chromatography A **915**, 1 (2001).

[30] N. Shimizu, T. Mizusaki, Y. Utsuno, and Y. Tsunoda, Computer Physics Communications **244**, 372 (2019).

[31] R. Machleidt, Phys. Rev. C **63**, 024001 (2001).

[32] S. Bonger, T. Kuo, and L. Coraggio, Nuclear Physics A **684**, 432 (2001), few-Body Problems in Physics.

[33] L. Coraggio, A. Covello, A. Gargano, N. Itaco, and T. Kuo, Annals of Physics **327**, 2125 (2012).

[34] J. M. Allmond, D. C. Radford, C. Baktash, J. C. Batchelder, A. Galindo-Uribarri, C. J. Gross, P. A. Hausladen, K. Lagergren, Y. Larochelle, E. Padilla-Rodal, and C.-H. Yu, Phys. Rev. C **84**, 061303 (2011).